

This is the author-created version of the following work:

Joyce, K.E., Duce, S., Leahy, S.M., Leon, J., and Maier, S.W. (2019) *Principles and practice of acquiring drone-based image data in marine environments. Marine and Freshwater Research*, 70 (7) pp. 952-963.

Access to this file is available from:

<https://researchonline.jcu.edu.au/54529/>

Published Version: © CSIRO 2019. Accepted Version may be made open access is an Institutional Repository without embargo.

Please refer to the original source for the final version of this work:

<https://doi.org/10.1071/MF17380>

1 **Principles and practice of acquiring drone-based image data in marine environments**

2 *K. E. Joyce^{A,D}, S. Duce^A, S. M. Leahy^A, J. Leon^B and S. W. Maier^C*

3 ^ACollege of Science and Engineering, James Cook University, Macgregor Rd, Smithfield 4870,
4 Queensland, Australia

5 ^BSchool of Science and Engineering, University of the Sunshine Coast, Sippy Downs 4556,
6 Queensland, Australia

7 ^Cmaitec, PO Box U19, Charles Darwin University 0815 Northern Territory, Australia.

8 ^DCorresponding author. Email: karen.joyce@jcu.edu.au

9 With almost limitless applications across marine and freshwater environments, the number of people using, and
10 wanting to use, remotely piloted aircraft systems (or drones) is increasing exponentially. However, successfully
11 using drones for data collection and mapping is often preceded by hours of researching drone capabilities and
12 functionality followed by numerous limited-success flights as users tailor their approach to data collection
13 through trial and error. Working over water can be particularly complex and the published research using drones
14 rarely documents the methodology and practical information in sufficient detail to allow others, with little
15 remote pilot experience, to replicate them or to learn from their mistakes. This can be frustrating and expensive,
16 particularly when working in remote locations where the window of access is small. The aim of this paper is to
17 provide a practical guide to drone-based data acquisition considerations. We hope to minimise the amount of
18 trial and error required to obtain high-quality, map-ready data by outlining the principles and practice of data
19 collection using drones, particularly in marine and freshwater environments. Importantly, our recommendations
20 are grounded in remote sensing and photogrammetry theory so that the data collected are appropriate for making
21 measurements and conducting quantitative data analysis.

22 With almost limitless applications across marine and freshwater environments, the number of people using, and
23 wanting to use, drones is rapidly increasing. However, what appears simple at first glance can often become
24 complicated when quantitative data collection is required. In this paper we provide a practical guide to drone-
25 based data acquisition considerations, particularly in marine and freshwater environments.

26 MF17380

27 *K. E. Joyce et al.*

28 Using drones in marine environments

29 **Additional keywords:** high resolution, thermal, three-dimensional mapping, unmanned aerial system (UAS),
30 unmanned aerial vehicle (UAV).

31 **Introduction**

32 Improvements in satellite technology over the past 20 years have markedly increased the value of
33 remote sensing imagery to ecologists (Goodman *et al.* 2013). Yet, with a best ground resolution of 31
34 cm per pixel for panchromatic and 1.24 m for multispectral data (Worldview-3 satellite), commercial

35 satellite imagery remains best suited to assessing benthic condition and change at the scale of entire
36 reefs or reef systems (Hamylton 2017a, 2017b; Roelfsema *et al.* 2018); it struggles to provide the
37 level of detail relevant to biologists and reef managers, who are often interested in benthic condition
38 with significantly finer detail, even down to the scale of individual organisms, plants or colonies (e.g.
39 Perry *et al.* 2012; Richardson *et al.* 2017). At the other extreme, in-water visual or photographic
40 surveys by snorkel or SCUBA can provide this extremely detailed data on reef condition and benthic
41 cover, but their coverage is limited to transects of tens to hundreds of metres (e.g. Leon *et al.* 2015;
42 Chennu *et al.* 2017). Furthermore, the data collected during in-water surveys is traditionally not
43 spatially explicit (Murphy and Jenkins 2010). This means that although researchers can provide, for
44 example, average differences in percentage benthic cover through time, it is often not possible to
45 pinpoint exactly where the changes have occurred. Importantly, determining the ‘where’ is a critical
46 first step in being able to assess the ‘why’ behind changes occurring in an ecosystem (Hamylton
47 2017a, 2017b).

48 Drone technology fits squarely between these two approaches (Fig. 1). Drones (also called
49 remotely piloted aircraft systems (RPASs) or unmanned aerial vehicles (UAVs)) provide the same
50 continuous overhead or ‘eye in the sky’ perspective as satellites. However, because they operate at a
51 much lower altitude, drones can capture considerably more detailed imagery with pixel sizes in the
52 order of centimetres depending on flying height (Berni *et al.* 2009a, 2009b; Dunford *et al.* 2009;
53 Flynn and Chapra 2014). In addition, drones can collect imagery under conditions where satellites
54 would be of limited use, such as high cloud cover. Drones also offer greater flexibility in the timing
55 and frequency of image capture, allowing users to capture images at a certain tide stage (e.g. low tide;
56 see Casella *et al.* 2017) or before and after events (e.g. storms; see Ierodiaconou *et al.* 2016). Where
57 in-water surveys are limited in their coverage, drones can survey significantly larger areas while still
58 providing high-resolution information, with the added benefit of being spatially explicit and highly
59 replicable (Hamylton 2017a, 2017b). In short, drones are powerful additions to data collection
60 protocols, particularly in marine science.

61 The advantages of drones have been well documented across a range of disciplines, including
62 agriculture (e.g. Herwitz *et al.* 2004; Berni *et al.* 2009a, 2009b; Xiang and Tian 2011), emergency
63 management (e.g. Ambrosia *et al.* 2005), terrestrial ecology and wildlife conservation (e.g. Laliberte
64 *et al.* 2011; Wallace *et al.* 2012; Gonzalez *et al.* 2016) and marine science (e.g. Hodgson *et al.* 2013;
65 Casella *et al.* 2017). These advantages include the ability to cheaply and frequently collect high-
66 resolution imagery across reasonably large areas that may be otherwise inaccessible or dangerous.
67 However, in order to collect more than just ‘pretty pictures’, there are certain principles to follow and
68 the associated challenges are not always well documented in the scientific literature. So, how can
69 researchers incorporate this powerful, and increasingly accessible, new technology into research or
70 monitoring programs? This paper provides practical advice on the principles and practice of using

71 drones for numerous applications in terrestrial and aquatic environments. We describe some valuable
72 marine applications of drone imagery and explain the basics of drone set-up and operation, survey
73 design and safety precautions.

74 **Marine applications**

75 The type of information that can be detected by drones is limited primarily by their payload
76 capacity. Sensor miniaturisation, in combination with increased payload capacity and battery life of
77 small drones (<25 kg), now makes it feasible for researchers to collect data beyond the visible
78 spectrum captured by traditional cameras. Coupled with the high spatial resolution and controlled
79 flight path unique to drone operation, this is a considerable advance in terms of collecting data and
80 ultimately providing information in marine environments (Murfitt *et al.* 2017). Below we highlight
81 just a few of the most common uses.

82 *Two-dimensional habitat mapping*

83 At its most basic, drone imagery can be used to visualise a study site, including benthic
84 composition (Chirayath and Earle 2016) and local fauna, and their use of the space (for a thorough
85 review of this topic, see Colefax *et al.* 2018). These applications are analogous to the site overviews
86 and animal surveys traditionally conducted using low airplane or helicopter flyovers (e.g. Rowat *et al.*
87 2009; Duke *et al.* 2017; Hughes *et al.* 2017; Sheldon *et al.* 2017). However, for many researchers,
88 hiring manned aircraft is prohibitively expensive. Even with expert staff, manned aircraft flyovers do
89 not necessarily generate the concrete, shareable, quantitative images that are crucial to providing a
90 baseline against which to assess future surveys (Colefax *et al.* 2018).

91 Downward-facing (nadir) imagery from one or more drone flights can be stitched together to
92 produce image mosaics, or orthomosaics, if the images are geometrically corrected to remove any
93 spatial distortions. With the assistance of an on-board global positioning system (GPS) and
94 supplemented, where possible, with ground control points, the data can also be georeferenced (i.e.
95 located in geographic space with known x and y coordinates). For many marine researchers, a mosaic
96 of visible light imagery alone can provide a helpful context to their study sites (Chirayath and Earle
97 2016). Image data processing using colour information alone, or using colour with shape, size, texture
98 and context information from protocols such as object-based image analysis, can be used to generate
99 habitat maps to better understand the magnitude and location of the changes that are occurring on
100 coral reefs (Leon and Woodroffe 2011; Wahidin *et al.* 2015; Fig. 2). Although both drone and in-
101 water visual surveys can quantify benthic composition, drone imagery is spatially explicit, providing
102 information on the relative location and distribution patterns of benthic components (Chirayath and
103 Earle 2016), as well as serving as a geolocated baseline against which to align and carry out future
104 surveys.

105 *Three-dimensional habitat complexity models*

106 Habitat complexity or rugosity is a crucial aspect for ecology, but can be difficult to assess at
107 appropriate spatial scales (Kovalenko *et al.* 2012). Benthic habitat complexity is traditionally assessed
108 by determining the length of chain required to drape over a horizontal length of 1 m on the reef (Risk
109 1972; Alvarez-Filip *et al.* 2009). However, chain placement can be subjective, painstaking and
110 damaging to corals. Benthic habitat complexity can be assessed more rapidly using a relative index,
111 but this provides a coarser metric of rugosity and, at times, can be subject to observer bias
112 (McCormick 1994). Regardless of the technique, benthic habitat complexity is a highly heterogeneous
113 characteristic, which means multiple measurements must be taken in order to gain an accurate
114 representation of true rugosity (Storlazzi *et al.* 2016). It is therefore incredibly labour intensive.

115 Alternatively, considerable research has now been undertaken to assess the benefits of
116 photogrammetry for measuring rugosity (e.g. Friedman *et al.* 2012; Figueira *et al.* 2015; Storlazzi *et*
117 *al.* 2016). Collecting imagery of a site (whether by drone, autonomous underwater vehicle or using in-
118 water hand-held cameras) with high levels of overlap and sidelap (sometimes called forward and
119 lateral overlap) between images allows every visible part of the benthos to be perceived from a range
120 of angles. This means that high-resolution three-dimensional models of the benthos can then be
121 generated using structure from motion (SfM) algorithms (Leon *et al.* 2015; Casella *et al.* 2017; Fig.
122 2). These high-resolution benthic complexity maps are permanent records of a site's benthic
123 complexity, and can be revisited in combination with habitat maps of live coral cover, or in time
124 series to identify degradation or improvements in benthic rugosity. They can even be subsampled at a
125 range of resolutions to identify the scale of benthic complexity of functional importance to different
126 taxa (Richardson *et al.* 2017). This method of quantifying benthic complexity can also be compared
127 directly with traditional methods of in-water complexity measures to assess the accuracy of staff
128 undergoing field training, or to calibrate a transitional period from using in-water to imagery-based
129 methods when contributing to long-term datasets. Furthermore, this image-based approach using SfM
130 is entirely non-intrusive and will not damage the benthic habitat (Ferrari *et al.* 2016).

131 Drone imagery and SfM algorithms have been widely and successfully used to derive XYZ point
132 clouds in terrestrial applications (Smith *et al.* 2016; Marteau *et al.* 2017; Kalacska *et al.* 2017;
133 Mlambo *et al.* 2017). However, underwater applications of photogrammetric measurements need to
134 account for two additional limitations. The first is water clarity, limiting the application of
135 photogrammetry to areas with calm (i.e. no wave turbulence) and very clear waters, such as offshore
136 coral reefs. The second challenge is light refraction as it crosses the air–water interface (Chirayath and
137 Earle 2016; Casella *et al.* 2017). Refraction correction techniques, such as the simplified version of
138 Snell's Law for nadir SfM imagery proposed by Woodget *et al.* (2015) or the multicamera refraction
139 correction proposed by Dietrich (2017), go some way towards overcoming this challenge. Maas
140 (2015) also presented an elegant model to reduce the degradation of geometric accuracy in underwater

141 photogrammetry, but current off-the-shelf photogrammetry software packages do not provide such
142 solutions as yet. Fluid lensing technology, presented by [Chirayath and Earle \(2016\)](#), also potentially
143 offers a novel solution to distortions caused by the water column, but is still limited to use in clear,
144 shallow water (<10 m) and requires extreme computer processing. For the above reasons, realistic use
145 of SfM from drone imagery of submerged environments is limited to exceptionally calm, clear days
146 with minimal water overlaying the features of interest. Alternatively, underwater SfM may be
147 appropriate.

148 *Sea surface temperature and animal monitoring*

149 Currently, remotely sensed thermal data is acquired by satellites such as NASA's Landsat 8, which
150 has a pixel size of 100 m and a revisit frequency of 16 days. Alternatively, the moderate-resolution
151 imaging spectroradiometer (MODIS) sensor on the Terra satellite acquires data daily, but with a 1-km
152 pixel size. These spatial and temporal resolutions are valuable for capturing thermal patterns at global
153 and regional scales, but are not able to elucidate the spatial heterogeneity in the thermal experiences
154 of individual coral colonies. Thermal information at finer scales is required to understand events such
155 as coral bleaching. Although an array of in-water temperature loggers could conceivably collect sea
156 surface temperature (SST) data at the fine scale most relevant to coral bleaching ([Gorospe and Karl
2011](#)), such a system is expensive, labour intensive to deploy and unreasonable to move between
158 study sites. Furthermore, such point-based data collection requires predictive modelling to 'fill the
159 gaps' between individual points in the array, whereas remotely sensed imagery provides spatially
160 contiguous data that can be readily collected and compared among several study sites. In our
161 experience, drone-mounted thermal sensors can collect contiguous relative SST imagery with a
162 ground sample distance of 6–12 cm ([Fig. 3](#)), depending on flight altitude and the resolution of the
163 camera itself. Similar work has also been conducted by [Lee et al. \(2016\)](#), who demonstrated the
164 benefit of using drone-based SST imagery for mapping groundwater discharge. Repeated imaging
165 through time may elucidate fine-scale water circulation patterns, particularly when used in
166 conjunction with the three-dimensional benthic rugosity models described above. However,
167 calibration and validation of thermal sensors for absolute temperatures is challenging, and this work is
168 the subject of a follow-up publication (Maier and Joyce, in prep).

169 An important limitation of remotely sensed SST data, be it from satellites or drones, is the depth to
170 which temperature can actually be detected. Observations by infrared sensors are essentially limited to
171 the top 10 μm of a waterbody, often referred to as water 'skin' temperature ([Kunzer and Dech 2013](#)).
172 In well-mixed systems, skin temperature is closely related to temperature at greater depths (e.g. 1 cm,
173 50 cm, 1 m, 5 m). Temperature as a function of depth must then be modelled, using *in situ*
174 measurements, to convert remotely sensed skin temperature to SSTs at depths that are meaningful for
175 corals and other undersea organisms.

176 In addition, remotely sensed thermal data are highly dependent on the thermal emissivity properties
177 of the material being imaged (i.e. how effective it is at emitting energy as thermal radiation). For
178 example, water, with its high emissivity coefficient (~0.95, depending on its composition), will
179 always appear warmer in thermal images than steel (emissivity 0.23–0.83, depending on age and
180 surface tarnish), even if the two materials are at the same true temperature. As such, quantitative
181 thermal imaging is best applied to homogeneous landscapes (e.g. water), unless users are prepared to
182 carry out material-specific emissivity corrections on the dataset (Kunzer and Dech 2013).

183 Drone-mounted thermal cameras can also be used for spatially extensive and non-invasive animal
184 observations, such as identifying and counting seals (Seymour *et al.* 2017), as long as safe and legal
185 minimum distances from these animals are respected (Junda *et al.* 2015). Owing to the low energy
186 levels of electromagnetic radiation in the thermal infrared range, users should expect the ground
187 sample distance of thermal cameras to be coarser than visible light cameras flown at the same altitude.
188 The size of the animal or feature of interest must be taken into account when identifying the required
189 image pixel size, and therefore drone flight height.. As a whole, thermal imaging offers great potential
190 to enrich faunal surveys, and is particularly suited to areas where human access is limited, either
191 logistically or for safety reasons (McCafferty 2007; Gonzalez *et al.* 2016).

192 Thermal cameras are often best operated at night to avoid sunlight contamination and to more
193 clearly identify nested or nocturnal animals. However, be aware that night-time flight may also
194 require additional certification from airspace governing authorities.

195 **Building drone capability**

196 Building an organisation's, or an individual's, drone capability (i.e. the ability to successfully
197 collect data using drones) takes planning, time and money. Fig. 4 shows a typical workflow for drone-
198 based data collection from preparation through to surveying. Estimated time frames are provided, as
199 well as references to the location in this paper of further information on each of the steps.

200 *Application requirements*

201 In some cases, drones are seen to be a solution looking for a problem. It is therefore important to
202 understand the conditions under which they are best used and the type of information that they are
203 suitable for providing. Before determining whether drones are appropriate for any particular
204 application, the user should return to some remote sensing fundamentals that drive the selection of
205 optimal image datasets. This will determine the sensor and drone infrastructure that is required to
206 achieve the end goal (Fig. 5, information requirements).

207 *Logistical considerations*

208 Several logistical and administrative protocols are inherent to the use of drones, including staff
209 training and licencing, liability insurance and guidelines or permits for operating in areas such as the

210 Great Barrier Reef Marine Park. Jurisdiction-specific regulations restrict drone-based activities in
211 national parks, around marine mammals and other areas of wildlife activity, such as seabird nesting
212 and foraging. Care should also be taken to minimise the chance of drone–wildlife interactions in
213 general through the selection of suitable take-off and landing zones, altering flight timing or adopting
214 specific flight techniques, such as those documented by [Junda *et al.* \(2015\)](#). The comprehensive
215 review by [Mulero-Pazmany *et al.* \(2017\)](#) on the effect of drones on wildlife clearly demonstrates the
216 need for a sit- specific plan that takes into account the time of day, type of wildlife in the area and size
217 of drone to be flown.

218 When considering whether to incorporate drone-collected imagery into your work, it is important to
219 identify trade-offs and where you may be willing to compromise. For example, as drones increase in
220 size and expense, generally they will be able to provide higher-quality data (spatially, spectrally, or
221 both) over larger areas. However, an increase in size also introduces challenges with battery
222 transportation and may require special protocols for transporting ‘dangerous goods’. Larger drones
223 may require an additional licence for remote pilots and can be cumbersome to operate, particularly if
224 considering boat-based launch and retrieval.

225 As a general rule, fixed-wing aircraft are more efficient than rotary and are able to survey larger
226 areas ([Floreano and Wood 2015](#)). However, they require large areas for take-off and landing that may
227 not suit many marine operations. As a compromise between fixed-wing and rotary drones, recent
228 progression in vertical take-off and land (VTOL) drone technology ([Watts *et al.* 2012](#)) is an exciting
229 step forward for marine applications in the future. All things considered, for ease of operation, safety
230 and budget, users should consider the smallest and cheapest drone that will satisfy their mission
231 requirements.

232 Finally, it is important for all staff to have appropriate equipment and training to monitor radio
233 channels and airspace for other users, particularly manned aircraft such as seaplanes and helicopters.

234 *Flight planning*

235 To achieve the best orthomosaics, users should aim to keep the survey area to a square or rectangle
236 shape. Because mosaic products tend to decrease in accuracy towards the edges where overlap and
237 sidelap between images decreases, the rectangular shape maximises the area of high-quality processed
238 data. The survey area should be larger than the actual region of interest to ensure all of it is captured
239 near nadir (i.e. where there is minimal distortion at the centre of each contributing photographic
240 frame) with the required level of overlap and sidelap. To create three-dimensional surface models, it is
241 important to capture an area even larger still, to capture off-nadir views from all directions. As much
242 as 90% overlap and 85% sidelap can be required for these applications to ensure that the appropriate
243 number of tie points between images can be found. We have found this high overlap to be particularly
244 important when mapping submerged features and contending with sun glint and partially obscured

245 features (see below). Recommended overlap and sidelap are target and software dependent, so we
246 refer the reader to user manuals of software, such as Pix4D (www.support.pix4d.com, accessed 21
247 May 2017) or Agisoft Photoscan (www.agisoft.com, accessed 21 May 2017). To assist in planning,
248 **Fig. 6** shows how the ground sampling distance (i.e. the area of the ground covered by each pixel) is
249 influenced by flight altitude. Flight planning software automatically calculates flight paths over the
250 defined study area based on user-specified inputs of flying altitude, desired overlap and sidelap and
251 sensor characteristics. The software will predict the flying time required to complete the mission.
252 Based on this time and your knowledge of your drone's battery capabilities, you can determine how
253 many flights will be necessary to cover the study area. Remember that operational battery life is lower
254 than the maximum flight time specified in the manual, which is measured under 'ideal' conditions
255 with no reserve. In addition, batteries do not discharge at an even rate, with the discharge rate
256 increasing markedly below a certain level (**Traub 2016**). It is important to allow yourself a safety
257 buffer to return and land safely even if unforeseen circumstances arise. Wind and payload will also
258 affect how long the drone's battery lasts. Always aim to land with a minimum of 25% battery life and
259 closely monitor the battery level using your ground control system (remote control, tablet or laptop)
260 as you fly.

261 *Considerations specific to working over water*

262 As outlined above, working with drones over water can yield extremely valuable data about a range
263 of variables, sometimes unobtainable by any other means. However, working over water requires
264 some additional considerations and planning to ensure the success of the mission. Two major factors
265 affect the quality of images acquired during a survey of submerged features: sun glint and subsurface
266 illumination (**Mount 2005**). Sun glint (or sun glitter) occurs when light is reflected back to the sensor
267 by the surface of the water, obscuring what is beneath it (e.g. **Fig. 7**). It presents a significant
268 challenge when capturing drone imagery of aquatic environments (**Flynn and Chapra 2014**). However,
269 the extent to which sun glint affects the resultant mosaic can be managed and overcome with careful
270 flight planning (**Mount 2005**). We believe that it is best to avoid glint contamination in the first place,
271 rather than have to correct the imagery during postprocessing. To do this, the main considerations are
272 time of image capture (and corresponding solar position), flight direction and camera angle.

273 Solar position during image capture is important. The solar azimuth is a measure of where in the
274 sky the sun is or will be located. It is measured in degrees clockwise from north for a given observer
275 point at a given time (**Fig. 8**). The elevation angle (also called the altitude angle or sun angle) refers to
276 the position of the sun in the sky as an angle from the horizon (i.e. at sunrise, the sun elevation angle
277 will be 0°). As a general rule, sun glint will be minimal when imagery is captured when sun elevation
278 is less than 35° (**Mount 2005**; i.e. early in the morning). Avoiding mapping missions over water
279 around midday will ensure the glint of reflected sunlight is on the edge of imagery rather than the
280 centre, and therefore can be more easily removed during imagery processing. However, this limits the

281 amount of light available and reduces the depth to which imagery is effective, and can result in strong
282 shadowing in images of three-dimensional surfaces. It also restricts the time available to capture
283 imagery and may not fit with tide and other logistical considerations.

284 To capture good-quality imagery when the sun is higher in the sky, the flight path should be
285 planned such that the drone is flying either directly towards or away from the sun azimuth (i.e. the
286 azimuth $\pm 180^\circ$). Fig. 8 shows how to calculate the optimal flight direction based on solar position.
287 Either direction is fine if the sensor is at nadir (pointing vertically straight down), but the drone
288 orientation in flight should be kept constant across the flight in order to more easily crop sun glint
289 effects across all the photographs taken during the flight. This is simple when using a multirotor
290 drone, although it is not possible to fly backwards with a fixed wing. If using the latter, it may be
291 necessary to only obtain imagery every second flight line, or to apply alternating cropping algorithms
292 to alternating flight lines. Alternatively, tilting the camera angle slightly off nadir will reduce and
293 move glint to the edges of the imagery so that it has less effect on the mosaicked product (Fig. 7). We
294 have found an off-nadir angle of 15° to be an acceptable compromise between reducing glint and
295 introducing oblique distortions to imagery. Geometric error will be introduced because of the off-
296 nadir imagery, but high degrees of overlap (oversampling) will help mitigate this (Flynn and Chapra
297 2014). Georeferencing after mosaicking will most likely also be necessary. Further, if a camera is
298 angled slightly off nadir, then drone orientation in flight should always be directly away from the sun
299 (i.e. in the direction of sun azimuth $\pm 180^\circ$). This means that the drone will be flying backwards for
300 half the survey. Several online services are available to calculate the sun azimuth and elevation angle
301 for a given location at a given time, such as Geoscience Australia's sun and moon position calculator
302 (<http://www.ga.gov.au/geodesy/astro/smpos.jsp>, accessed 21 May 2018).

303 It is possible to check the imagery on your ground station (i.e. tablet or smartphone) as you are
304 capturing it to find the balance between oblique (off-nadir) capture and minimal glint. Collecting
305 oblique imagery has implications on the ground sampling distance (GSD) with pixels covering a
306 smaller area in the foreground than the background of an image (Hohle 2008; Pepe and Preszioso
307 2016) and can make processing more difficult (Grenzdörffer *et al.* 2008). Indeed, Casella *et al.* (2017)
308 note that bathymetric reconstruction works better on images taken at nadir because peripheral areas of
309 a scene are more strongly affected by water refraction.

310 Even with a slight camera tilt and optimal flight direction, sun glint may still appear in individual
311 images. However, if the glint is towards the edge of an image, a high-quality orthomosaic can be
312 created if high levels of overlap and sidelap are achieved (Fig. 7). If the drone is continually capturing
313 imagery while it is flying (as opposed to hovering for capture), increasing the frontlap will not affect
314 the area of coverage or the time taken to complete the flight. This holds true until such a frequency
315 where the camera focus, capture and save process are no longer able to keep up with the speed of the
316 drone in flight. However, increasing the sidelap will certainly reduce areal coverage. Regardless of

317 glint, increasing frontlap and sidelap will lead to a higher-quality mosaic and digital surface model. If
318 glint is unavoidable at the time of image capture and persists through the mosaicking process, a
319 simple post-processing routine may be an option if a camera with a near-infrared sensor has been used
320 (Hochberg *et al.* 2003).

321 Using polarising filters or working on a cloudy day with diffuse light are alternatives that reduce
322 sun glint at the time of image capture. However, working on a cloudy day means the amount of light
323 reaching the subsurface will be reduced. The level to which this affects available light will, of course,
324 depend on the cloud thickness and time of day. On cloudy days, capturing data closer to midday when
325 the sun is at full strength can be a viable compromise (Kay *et al.* 2009).

326 It is important to also consider water quality, wind and sea state when planning image collection
327 flights. Certain aquatic environments lend themselves better to aerial mapping than others. Low-
328 turbidity conditions and shallow regions are best, even better if they are tidally exposed. The presence
329 of waves or surface ripples can hinder subsurface visibility in imagery (Mount 2005). Although most
330 commercially available drones are able to fly in winds up to 20 knots, wind speeds greater than ~5–10
331 knots ($2.5\text{--}5\text{ m s}^{-1}$) can create ripples and waves on the water surface that limit image quality (Mount
332 2005).

333 When launching a drone from a boat, remember that the boat may move on its anchor during your
334 survey. If the boat moves during your flight, the ‘home’ location stored by your drone before it takes
335 off may be over the water. It is possible to create a dynamic home, whereby the drone continually
336 updates the home location based on that of the controller. However, in case of lost connectivity
337 between drone and controller, this can be erroneous and manual landing is preferable.

338 *Accuracy and ground control*

339 As with all remotely sensed data and mapping products, appropriate geometric processing and
340 georeferencing are required to position the image, derive accurate measurements, such as distance,
341 perimeter, area and elevation, and to perform precise change detection analyses. Although drones do
342 have on-board GPS units that can be used to tag images with coordinates at the time of image capture,
343 their accuracy is typically approximately $\pm 5\text{ m}$, depending on the specific unit itself as well as the
344 satellite configuration and atmospheric conditions at the time of acquisition. Further errors can be
345 introduced if the camera is pointed off nadir so that the area it images does not necessarily correspond
346 to the GPS location of the drone. This means that without additional ground control, it is not possible
347 to derive highly accurate absolute measurements of location, area, height, volume or changes in any
348 of these parameters.

349 If accurate and absolute XYZ measurements are mission critical, ground control points (GCPs)
350 must be deployed and their location recorded within the survey area. The number and spatial
351 distribution of GCPs and the capability of the GPS unit used have important effects on the accuracy of

352 results (James *et al.* 2017). Many studies suggest using between 10 and 20 GCPs (Clapuyt *et al.* 2016;
353 Tonkin and Midgley 2016). However, there will be a trade-off between what is desirable and what is
354 realistically achievable.

355 To achieve accurate absolute measures of vertical elevation a survey-grade total station or real-time
356 kinematic differential GPS (1-cm horizontal and 2-cm vertical accuracy) is required to position the
357 GCPs (Harwin and Lucieer 2012). This equipment is expensive and can only be used in intertidal or
358 shallow areas (e.g. Bryson *et al.* 2016) because receivers do not work underwater. Indeed, laying out
359 and accurately surveying GCPs is challenging, particularly underwater, and in many cases is not
360 feasible. Where survey-grade positioning equipment is not available, GCPs can be configured in a
361 triangle with each side of a known length (e.g. Bryson *et al.* 2013). This allows for absolute scaling
362 corrections within the image (i.e. distances, areas and volumes can be accurately and precisely
363 calculated; Bryson *et al.* 2013). Where drones are used to survey an inaccessible area, collecting
364 GCPs may not be possible at all. In these cases, the accuracy limitations of the on-board GPS must be
365 taken into account when presenting and interpreting the results, but will not preclude data collection
366 or analysis.

367 *Calibrating and validating*

368 In some cases it may be appropriate to use drone imagery as a source of *in situ* data for ground
369 truthing (calibration, validation, or both) of coarser-scale products such as satellite data. However, in
370 other instances the drone data itself should be ground truthed. We suggest that calibration and
371 validation of drone imagery based on field measurements may be required in the following
372 circumstances:

- 373 • when the features of interest in a submerged environment may be partially obscured by the
374 intervening water column so there is uncertainty in identification due to light refraction or water
375 quality despite an otherwise high spatial resolution
- 376 • when undertaking quantitative mapping of variables where the absolute value of the variable of
377 interest needs to be measured and extrapolated (e.g. bathymetry, elevation, temperature,
378 biophysical variables)
- 379 • when the size of the feature of interest is smaller than or approaching the size of the ground
380 sampling distance (i.e. the pixel).

381 **Summary**

382 Using drones for a variety of research applications offers the opportunity to change our perspective
383 on the environment. In marine research, the advances offered by drones is arguably on par with the
384 extent to which SCUBA diving revolutionised underwater research 70 years ago. Incorporating drones
385 as legitimate research tools will empower scientists around the world to collect relevant, quantitative,

386 spatially explicit, extensive and replicable data for a range of terrestrial, marine and freshwater
387 habitats. However, we also caution that careful consideration of data acquisition and processing,
388 outlined herein, needs to be undertaken if drones are to move beyond the realm of providing ‘pretty
389 pictures’ and into delivering robust scientific and management information.

390 **Conflicts of interest**

391 The authors declare that they have no conflicts of interest

392 **Acknowledgements**

393 The authors’ work reported herein was supported by an Australian Research Council Linkage, Infrastructure,
394 Equipment, and Facilities (ARC LIEF) Grant LE150100181 to K. Joyce and S. Maier, a James Cook University
395 Development Grant and a Rising Star Grant to K. Joyce and University of Queensland Northern Great Barrier
396 Reef Habitat Mapping. Image mosaics were processed with Pix4D mapper Pro by Pix4D.

397 **References**

- 398 <jrn>Alvarez-Filip, L., Dulvy, N. K., Gill, J. A., Côté, I. M., and Watkinson, A. R. (2009). Flattening of
399 Caribbean coral reefs: region-wide declines in architectural complexity. *Proceedings of the Royal Society of*
400 *London – B. Biological Sciences* **276**(1669), 3019–3025. doi:10.98/rspb.2009.0339</jrn>
- 401 <conf>Ambrosia, V. G., Wegener, S. S., Brass, J. A., and Hinkley, E. (2005). Use of unmanned aerial vehicles
402 for fire detection. In ‘Proceedings of the 5th International Workshop on Remote Sensing and GIS
403 Applications to Forest Fire Management: Fire Effects Assessment’. (Eds J. De la Riva, F. Pérez-Cabello, and
404 E. Chuvieco.) pp. 9–17. (Universidad de Zaragoza, Zaragoza, Spain.)</conf>
- 405 <jrn>Bermi, J., Zarco-Tejada, P. J., Suarez, L., and Fereres, E. (2009a). Thermal and narrowband multispectral
406 remote sensing for vegetation monitoring from an unmanned aerial vehicle. *IEEE Transactions on*
407 *Geoscience and Remote Sensing* **47**(3), 722–738. doi:10.1109/TGRS.2008.2010457</jrn>
- 408 <jrn>Bermi, J. A. J., Zarco-Tejada, P. J., Sepulcre-Cantó, G., Fereres, E., and Villalobos, F. (2009b). Mapping
409 canopy conductance and cwsj in olive orchards using high resolution thermal remote sensing imagery.
410 *Remote Sensing of Environment* **113**(11), 2380–2388. doi:10.1016/j.rse.2009.06.018</jrn>
- 411 <jrn>Bryson, M., Johnson-Roberson, M., Murphy, R., and Bongiorno, D. (2013). Kite aerial photography for
412 low-cost, ultra-high spatial resolution multi-spectral mapping of intertidal landscapes. *PLoS One* **8**(9),
413 e73550. doi:10.1371/journal.pone.0073550</jrn>
- 414 <jrn>Bryson, M., Duce, S., Harris, D., Webster, J. M., Thompson, A., Vila-Concejo, A., and Williams, S. B.
415 (2016). Geomorphic changes of a coral shingle cay measured using kite aerial photography. *Geomorphology*
416 **270**, 1–8. doi:10.1016/j.geomorph.2016.06.018</jrn>
- 417 <jrn>Casella, E., Collin, A., Harris, D., Ferse, S., Bejarano, S., Parravicini, V., Hench, J. L., and Rovere, A.
418 (2017). Mapping coral reefs using consumer-grade drones and structure from motion photogrammetry
419 techniques. *Coral Reefs* **36**(1), 269–275. doi:10.1007/s00338-016-1522-0</jrn>

- 420 <jrn>Chennu, A., Färber, P., De'ath, G., de Beer, D., and Fabricius, K. E. (2017). A diver-operated
421 hyperspectral imaging and topographic surveying system for automated mapping of benthic habitats.
422 *Scientific Reports* **7**(7122), 1–12. </jrn>
- 423 <jrn>Chiabrando, F., Nex, F., Piatti, D., and Rinaudo, F. (2011). UAV and RPV systems for photogrammetric
424 surveys in archaeological areas: two tests in the Piedmont region (Italy). *Journal of Archaeological Science*
425 **38**, 697–710. doi:10.1016/j.jas.2010.10.022 </jrn>
- 426 <jrn>Chirayath, V., and Earle, S. A. (2016). Drones that see through waves – preliminary results from airborne
427 fluid lensing for centimetre-scale aquatic conservation. *Aquatic Conservation* **26**, 237–250.
428 doi:10.1002/aqc.2654 </jrn>
- 429 <jrn>Clapuyt, F., Vanacker, V., and Van Oost, K. (2016). Reproducibility of UAV-based earth topography
430 reconstructions based on structure-from-motion algorithms. *Geomorphology* **260**, 4–15.
431 doi:10.1016/j.geomorph.2015.05.011 </jrn>
- 432 <jrn>Colefax, A. P., Butcher, P. A., and Kelaher, B. P. (2017). The potential for unmanned aerial vehicles
433 (UAVs) to conduct marine fauna surveys in place of manned aircraft. *ICES Journal of Marine Science* **75**(1):
434 1–8. doi:10.1093/icesjms/fsx100 </jrn>
- 435 <jrn>Dandois, J. P., Olano, M., and Ellis, E. C. (2015). Optimal altitude, overlap, and weather conditions for
436 computer vision UAV estimates of forest structure. *Remote Sensing* **7**(10), 13895–13920.
437 doi:10.3390/rs71013895 </jrn>
- 438 <jrn>Dietrich, J. T. (2017). Bathymetric structure-from-motion: extracting shallow stream bathymetry from
439 multi-view stereo photogrammetry. *Earth Surface Processes and Landforms* **42**(2), 355–364.
440 doi:10.1002/esp.4060 </jrn>
- 441 <jrn>Duke, N. C., Kovacs, J. M., Griffiths, A. D., Preece, L., Hill, D. J. E., van Oosterzee, P., Mackenzie, J.,
442 Morning, H. S., and Burrows, D. (2017). Large-scale dieback of mangroves in Australia's Gulf of
443 Carpentaria: a severe ecosystem response, coincidental with an unusually extreme weather event. *Marine and*
444 *Freshwater Research* **68**(10), 1816–1829. doi:10.1071/MF16322 </jrn>
- 445 <jrn>Dunford, R., Michel, K., Gagnage, M., Piégay, H., and Trémelo, M. L. (2009). Potential and constraints of
446 unmanned aerial vehicle technology for the characterization of Mediterranean riparian forest. *International*
447 *Journal of Remote Sensing* **30**(19), 4915–4935. doi:10.1080/01431160903023025 </jrn>
- 448 <jrn>Ferrari, R., Bryson, M., Bridge, T., Hustache, J., Williams, S. B., Byrne, M., and Figueira, W. (2016).
449 Quantifying the response of structural complexity and community composition to environmental change in
450 marine communities. *Global Change Biology* **22**(5), 1965–1975. doi:10.1111/gcb.13197 </jrn>
- 451 <jrn>Figueira, W., Ferrari, R., Weatherby, E., Porter, A., Hawes, S., and Byrne, M. (2015). Accuracy and
452 precision of habitat structural complexity metrics derived from underwater photogrammetry. *Remote Sensing*
453 **7**(12), 16883–16900. doi:10.3390/rs71215859 </jrn>
- 454 <jrn>Floreano, D., and Wood, R. J. (2015). Science, technology and the future of small autonomous drones.
455 *Nature* **521**, 460–466. doi:10.1038/nature14544 </jrn>

- 456 <jrn>Flynn, K., and Chapra, S. (2014). Remote sensing of submerged aquatic vegetation in a shallow non-turbid
457 river using an unmanned aerial vehicle. *Remote Sensing* **6**(12), 12815–12836. doi:10.3390/rs61212815</jrn>
- 458 <jrn>Friedman, A., Pizarro, O., Williams, S. B., and Johnson-Roberson, M. (2012). Multi-scale measures of
459 rugosity, slope and aspect from benthic stereo image reconstructions [published erratum appears in *PLoS One*
460 2013; **8**(12): doi:10.1371/annotation/55ee98d1-6731-4bee-81d6-03ce0259c191]. *PLoS One* **7**(12), e50440.
461 doi:10.1371/journal.pone.0050440</jrn>
- 462 <jrn>Gonzalez, L., Montes, G., Puig, E., Johnson, S., Mengersen, K., and Gaston, K. (2016). Unmanned aerial
463 vehicles (UAVs) and artificial intelligence revolutionizing wildlife monitoring and conservation. *Sensors*
464 **16**(1), 97. doi:10.3390/s16010097</jrn>
- 465 <bok>Goodman, J. A., Purkis, S. J., and Phinn, S. R. (2013). ‘Coral Reef Remote Sensing. A Guide for
466 Mapping, Monitoring, and Management.’ (Springer: Netherlands.)</bok>
- 467 <jrn>Gorospe, K. D., and Karl, S. A. (2011). Small-scale spatial analysis of in situ sea temperature throughout a
468 single coral patch reef. *Journal of Marine Biology* **2011**, 1–12. doi:10.1155/2011/719580</jrn>
- 469 <jrn>Grenzdörffer, G. J., Guretzki, M., and Friedlander, I. (2008). Photogrammetric image acquisition and
470 image analysis of oblique imagery. *The Photogrammetric Record* **23**(124), 372–386. doi:10.1111/j.1477.
471 9730.2008.00499.x</jrn>
- 472 <bok>Hamylton, S. (2017a). ‘Spatial Analysis of Coastal Environments.’ (Cambridge University Press:
473 Cambridge, UK.)</bok>
- 474 <jrn>Hamylton, S. M. (2017b). Mapping coral reef environments: a review of historical methods, recent
475 advances and future opportunities. *Progress in Physical Geography* **41**(6), 803–833.
476 doi:10.1177/0309133317744998</jrn>
- 477 <jrn>Harwin, S., and Lucieer, A. (2012). Assessing the accuracy of georeferenced point clouds produced via
478 multi-view stereopsis from unmanned aerial vehicle (UAV) imagery. *Remote Sensing* **4**(6), 1573–1599.
479 doi:10.3390/rs-4061573</jrn>
- 480 <jrn>Herwitz, S. R., Johnson, L. F., Dunagan, S. E., Higgins, R. G., Sullivan, D. V., Zheng, J., Lobitz, B. M.,
481 Leung, J. G., Gallmeyer, B. A., Aoyagi, M., Slye, R. E., and Brass, J. A. (2004). Imaging from an unmanned
482 aerial vehicle: agricultural surveillance and decision support. *Computers and Electronics in Agriculture*
483 **44**(1), 49–61. doi:10.1016/j.compag.2004.02.006</jrn>
- 484 <jrn>Hochberg, E. J., Andréfouët, S., and Tyler, M. R. (2003). Sea surface correction of high spatial resolution
485 ikonos images to improve bottom mapping in near-shore environments. *IEEE Transactions on Geoscience
486 and Remote Sensing* **41**(7), 1724–1729. doi:10.1109/TGRS.2003.815408</jrn>
- 487 <jrn>Hodgson, A., Kelly, N., and Peel, D. (2013). Unmanned aerial vehicles (UAVs) for surveying marine
488 fauna: a dugong case study. *PLoS One* **8**(11), e79556. doi:10.1371/journal.pone.0079556</jrn>
- 489 <jrn>Hohle, J. (2008). Photogrammetric measurements in oblique aerial images. *Photogrammetrie,
490 Fernerkundung, Geoinformation* **1**, 7–14.</jrn>

- 491 <jrn>Hughes, T. P., Kerry, J. T., Álvarez-Noriega, M., Álvarez-Romero, J. G., Anderson, K. D., Baird, A. H.,
492 Babcock, R. C., Beger, M., Bellwood, D. R., Berkelmans, R., Bridge, T. C., Butler, I. R., Byrne, M., Cantin,
493 N. E., Comeau, S., Connolly, S. R., Cumming, G. S., Dalton, S. J., Diaz-Pulido, G., Eakin, C. M., Figueira,
494 W. F., Gilmour, J. P., Harrison, H. B., Heron, S. F., Hoey, A. S., Hobbs, J.-P. A., Hoogenboom, M. O.,
495 Kennedy, E. V., Kuo, C.-y., Lough, J. M., Lowe, R. J., Liu, G., McCulloch, M. T., Malcolm, H. A.,
496 McWilliam, M. J., Pandolfi, J. M., Pears, R. J., Pratchett, M. S., Schoepf, V., Simpson, T., Skirving, W. J.,
497 Sommer, B., Torda, G., Wachenfeld, D. R., Willis, B. L., and Wilson, S. K. (2017). Global warming and
498 recurrent mass bleaching of corals. *Nature* **543**, 373–377. [doi:10.1038/nature21707](https://doi.org/10.1038/nature21707)</jrn>
- 499 <jrn>Ierodiaconou, D., Schimel, A. C. G., and Kennedy, D. M. (2016). A new perspective of storm bite on
500 sandy beaches using unmanned aerial vehicles. *Zeitschrift für Geomorphologie* **60**(3), 123–137.
501 [doi:10.1127/zfgf_suppl2016/0024](https://doi.org/10.1127/zfgf_suppl2016/0024)</jrn>
- 502 <jrn>James, M. R., Robson, S., d'Oleire-Oltmanns, S., and Niethammer, U. (2017). Optimising UAV
503 topographic surveys processed with structure-from-motion: ground control quality, quantity and bundle
504 adjustment. *Geomorphology* **280**, 51–66. [doi:10.1016/j.geomorph.2016.11.021](https://doi.org/10.1016/j.geomorph.2016.11.021)</jrn>
- 505 <jrn>Junda, J., Greene, E., and Bird, D. M. (2015). Proper flight technique for using a small rotary-winged
506 drone aircraft to safely, quickly, and accurately survey raptor nests. *Journal of Unmanned Vehicle Systems*
507 **3**(4), 222–236. [doi:10.1139/juvs-2015-0003](https://doi.org/10.1139/juvs-2015-0003)</jrn>
- 508 <jrn>Kalacska, M., Chmura, G., Lucanus, O., Bérubé, D., and Arroyo, P. (2017). Structure from motion will
509 revolutionize analyses of tidal wetland landscapes. *Remote Sensing of Environment* **199**, 14–24.
510 [doi:10.1016/j.rse.2017.06.023](https://doi.org/10.1016/j.rse.2017.06.023)</jrn>
- 511 <jrn>Kay, S., Hedley, J., and Lavender, S. (2009). Sun glint correction of high and low spatial resolution images
512 of aquatic scenes: a review of methods for visible and near-infrared wavelengths. *Remote Sensing* **1**(4), 697–
513 730. [doi:10.3390/rs1040697](https://doi.org/10.3390/rs1040697)</jrn>
- 514 <jrn>Kovalenko, K. E., Thomaz, S. M., and Warfe, D. M. (2012). Habitat complexity: approaches and future
515 directions. *Hydrobiologia* **685**(1), 1–17. [doi:10.1007/s10750-011-0974-z](https://doi.org/10.1007/s10750-011-0974-z)</jrn>
- 516 <other>Kunzer, C. and S. Dech (2013). Thermal infrared remote sensing. Sensors, methods, applications.
517 Springer, Netherlands. Doi: 10.1007/978-94-007-6639-6 537pp</other>
- 518 <jrn>Laliberte, A. S., Goforth, M. A., Steele, C. M., and Rango, A. (2011). Multispectral remote sensing from
519 unmanned aircraft: image processing workflows and applications for rangeland environments. *Remote*
520 *Sensing* **3**(11), 2529–2551. [doi:10.3390/rs3112529](https://doi.org/10.3390/rs3112529)</jrn>
- 521 <jrn>Lee, E., Yoon, H., Hyun, S. P., Burnett, W. C., Koh, D.-C., Ha, K., Kim, D.-j., Kim, Y., and Kang, K.-m.
522 (2016). Unmanned aerial vehicles (UAVs)-based thermal infrared (TIR) mapping, a novel approach to assess
523 groundwater discharge into the coastal zone. *Limnology and Oceanography, Methods* **14**(11), 725–735.
524 [doi:10.1002/lom3.10132](https://doi.org/10.1002/lom3.10132)</jrn>
- 525 <jrn>Leon, J., and Woodroffe, C. D. (2011). Improving the synoptic mapping of coral reef geomorphology
526 using object-based image analysis. *International Journal of Geographical Information Science* **25**(6), 949–
527 969. [doi:10.1080/13658816.2010.513980](https://doi.org/10.1080/13658816.2010.513980)</jrn>

- 528 <jrn>Leon, J. X., Roelfsema, C. M., Saunders, M. I., and Phinn, S. R. (2015). Measuring coral reef terrain
529 roughness using 'structure-from-motion' close-range photogrammetry. *Geomorphology* **242**, 21–28.
530 [doi:10.1016/j.geomorph.2015.01.030](https://doi.org/10.1016/j.geomorph.2015.01.030)</jrn>
- 531 <jrn>Maas, H.-G. (2015). On the accuracy potential in underwater/multimedia photogrammetry. *Sensors* **15**(8),
532 18140–18152. [doi:10.3390/s150818140](https://doi.org/10.3390/s150818140)</jrn>
- 533 Maier, S.W., and Joyce, K.E. (in prep). Accurate measurements with thermal imaging sensors on remotely
534 piloted aircraft: issues, challenges and solutions. *Remote Sensing of Environment*
- 535 <jrn>Marteau, B., Vericat, D., Gibbins, C., Batalla, R. J., and Green, D. R. (2017). Application of structure-
536 from-motion photogrammetry to river restoration. *Earth Surface Processes and Landforms* **42**(3), 503–515.
537 [doi:10.1002/esp.4086](https://doi.org/10.1002/esp.4086)</jrn>
- 538 <jrn>McCafferty, D. J. (2007). The value of infrared thermography for research on mammals: previous
539 applications and future directions. *Mammal Review* **37**(3), 207–223. [doi:10.1111/j.1365-2907.2007.00111.x](https://doi.org/10.1111/j.1365-2907.2007.00111.x)</jrn>
- 541 <jrn>McCormick, M. (1994). Comparison of field methods for measuring surface topography and their
542 associations with a tropical reef fish assemblage. *Marine Ecology Progress Series* **112**, 87–96.
543 [doi:10.3354/meps112087](https://doi.org/10.3354/meps112087)</jrn>
- 544 <jrn>Mlambo, R., Woodhouse, I., Gerard, F., and Anderson, K. (2017). Structure from motion (sfm)
545 photogrammetry with drone data: a low cost method for monitoring greenhouse gas emissions from forests in
546 developing countries. *Forests* **8**(3), 68. [doi:10.3390/f8030068](https://doi.org/10.3390/f8030068)</jrn>
- 547 <jrn>Mount, R. (2005). Acquisition of through-water aerial survey images: surface effects and the prediction of
548 sun glitter and subsurface illumination. *Photogrammetric Engineering and Remote Sensing* **71**(12), 1407–
549 1415. [doi:10.14358/PERS.71.12.1407](https://doi.org/10.14358/PERS.71.12.1407)</jrn>
- 550 <jrn>Mulero-Pázmány, M., Jenni-Eiermann, S., Strebel, N., Sattler, T., Negro, J. J., and Tablado, Z. (2017).
551 Unmanned aircraft systems as a new source of disturbance for wildlife: a systematic review. *PLoS One* **12**(6),
552 e0178448. [doi:10.1371/journal.pone.0178448](https://doi.org/10.1371/journal.pone.0178448)</jrn>
- 553 <jrn>Murfitt, S. L., Allan, B. M., Bellgrove, A., Rattray, A., Young, M. A., and Ierodiaconou, D. (2017).
554 Applications of unmanned aerial vehicles in intertidal reef monitoring. *Scientific Reports* **7**(1), 10259.
555 [doi:10.1038/s41598-017-10818-9](https://doi.org/10.1038/s41598-017-10818-9)</jrn>
- 556 <jrn>Murphy, H., and Jenkins, G. (2010). Observational methods used in marine spatial monitoring of fishes
557 and associated habitats: a review. *Marine and Freshwater Research* **61**, 236–252.
558 [doi:10.1071/MF09068](https://doi.org/10.1071/MF09068)</jrn>
- 559 <jrn>Peña, J. M., Torres-Sanchez, J., Serrano-Perez, A., de Castro, A. I., and Lopez-Granados, F. (2015).
560 Quantifying efficacy and limits of unmanned aerial vehicle (UAV) technology for weed seedling detection as
561 affected by sensor resolution. *Sensors* **15**(3), 5609–5626. [doi:10.3390/s150305609](https://doi.org/10.3390/s150305609)</jrn>
- 562 <conf>Pepe, M., and Preszioso, G. (2016). Two approaches for dense DSM generation from aerial digital
563 oblique camera system. In '2nd International Conference on Geographical Information Systems Theory,

- 564 Applications and Management', 26-27 Apr 2016, Rome, Italy) pp. 63–70. (Science and Technology
565 Publications: Setubal, Portugal.) </conf>
- 566 <jrn>Perroy, R. L., Sullivan, T., and Stephenson, N. (2017). Assessing the impacts of canopy openness and
567 flight parameters on detecting a sub-canopy tropical invasive plant using a small unmanned aerial system.
568 *ISPRS Journal of Photogrammetry and Remote Sensing* **125**, 174–183.
569 [doi:10.1016/j.isprsjprs.2017.01.018](https://doi.org/10.1016/j.isprsjprs.2017.01.018)</jrn>
- 570 <jrn>Perry, C. T., Edinger, E. N., Kench, P. S., Murphy, G. N., Smithers, S. G., Steneck, R. S., and Mumby, P.
571 J. (2012). Estimating rates of biologically driven coral reef framework production and erosion: a new census-
572 based carbonate budget methodology and applications to the reefs of Bonaire. *Coral Reefs* **31**(3), 853–868.
573 [doi:10.1007/s00338-012-0901-4](https://doi.org/10.1007/s00338-012-0901-4)</jrn>
- 574 <jrn>Richardson, L. E., Graham, N. A. J., and Hoey, A. S. (2017). Cross-scale habitat structure driven by coral
575 species composition on tropical reefs. *Scientific Reports* **7**(7557), 1–11.</jrn>
- 576 <jrn>Risk, M. J. (1972). Fish diversity on a coral reef in the Virgin Islands. *Atoll Research Bulletin* **153**, 1–4.
577 [doi:10.5479/si.00775630.153.1](https://doi.org/10.5479/si.00775630.153.1)</jrn>
- 578 <jrn>Roelfsema, C., Kovacs, E., Ortiz, J. C., Wolff, N. H., Callaghan, D., Wettle, M., Ronan, M., Hamylton, S.
579 M., Mumby, P. J., and Phinn, S. (2018). Coral reef habitat mapping: a combination of object-based image
580 analysis and ecological modelling. *Remote Sensing of Environment* **208**, 27–41.
581 [doi:10.1016/j.rse.2018.02.005](https://doi.org/10.1016/j.rse.2018.02.005)</jrn>
- 582 <jrn>Rowat, D., Gore, M., Meekan, M. G., Lawler, I. R., and Bradshaw, C. J. A. (2009). Aerial survey as a tool
583 to estimate whale shark abundance trends. *Journal of Experimental Marine Biology and Ecology* **368**(1), 1–8.
584 [doi:10.1016/j.jembe.2008.09.001](https://doi.org/10.1016/j.jembe.2008.09.001)</jrn>
- 585 <jrn>Seymour, A. C., Dale, J., Hammill, M., Halpin, P. N., and Johnston, D. W. (2017). Automated detection
586 and enumeration of marine wildlife using unmanned aircraft systems (UAS) and thermal imagery. *Scientific*
587 *Reports* **7**, 45127. [doi:10.1038/srep45127](https://doi.org/10.1038/srep45127)</jrn>
- 588 <other>Sheldon, K. E. W., Hobbs, R. C., Sims, C. L., Vate Brattstrom, L., Mocklin, J. A., Boyd, C., and
589 Mahoney, B. A. (2017). Aerial surveys of beluga whales (*Delphinapterus leucas*) in Cook Inlet, Alaska, June
590 2016. Alaska Fish Science Centre Processed Report 2017–09, NOAA, Seattle, WA, USA.</other>
- 591 <jrn>Smith, M. W., Carrivick, J. L., and Quincey, D. J. (2016). Structure from motion photogrammetry in
592 physical geography. *Progress in Physical Geography* **40**(2), 247–275. [doi:10.1177/0309133315615805](https://doi.org/10.1177/0309133315615805)</jrn>
- 593 <jrn>Storlazzi, C. D., Dartnell, P., Hatcher, G. A., and Gibbs, A. E. (2016). End of the chain? Rugosity and
594 fine-scale bathymetry from existing underwater digital imagery using structure-from-motion (sfm)
595 technology. *Coral Reefs* **35**(3), 889–894. [doi:10.1007/s00338-016-1462-8](https://doi.org/10.1007/s00338-016-1462-8)</jrn>
- 596 <jrn>Tonkin, T., and Midgley, N. (2016). Ground-control networks for image based surface reconstruction: an
597 investigation of optimum survey designs using UAV derived imagery and structure-from-motion
598 photogrammetry. *Remote Sensing* **8**(9), 786. [doi:10.3390/rs8090786](https://doi.org/10.3390/rs8090786)</jrn>

599 <jrn>Traub, L. (2016). Calculation of constant power lithium battery discharge curves. *Batteries* **2**(2), 17.
600 [doi:10.3390/batteries2020017](https://doi.org/10.3390/batteries2020017)</jrn>

601 <jrn>Wahidin, N., Siregar, V. P., Nababan, B., Jaya, I., and Wouthuyzen, S. (2015). Object-based image
602 analysis for coral reef benthic habitat mapping with several classification algorithms. *Procedia*
603 *Environmental Sciences* **24**, 222–227. [doi:10.1016/j.proenv.2015.03.029](https://doi.org/10.1016/j.proenv.2015.03.029)</jrn>

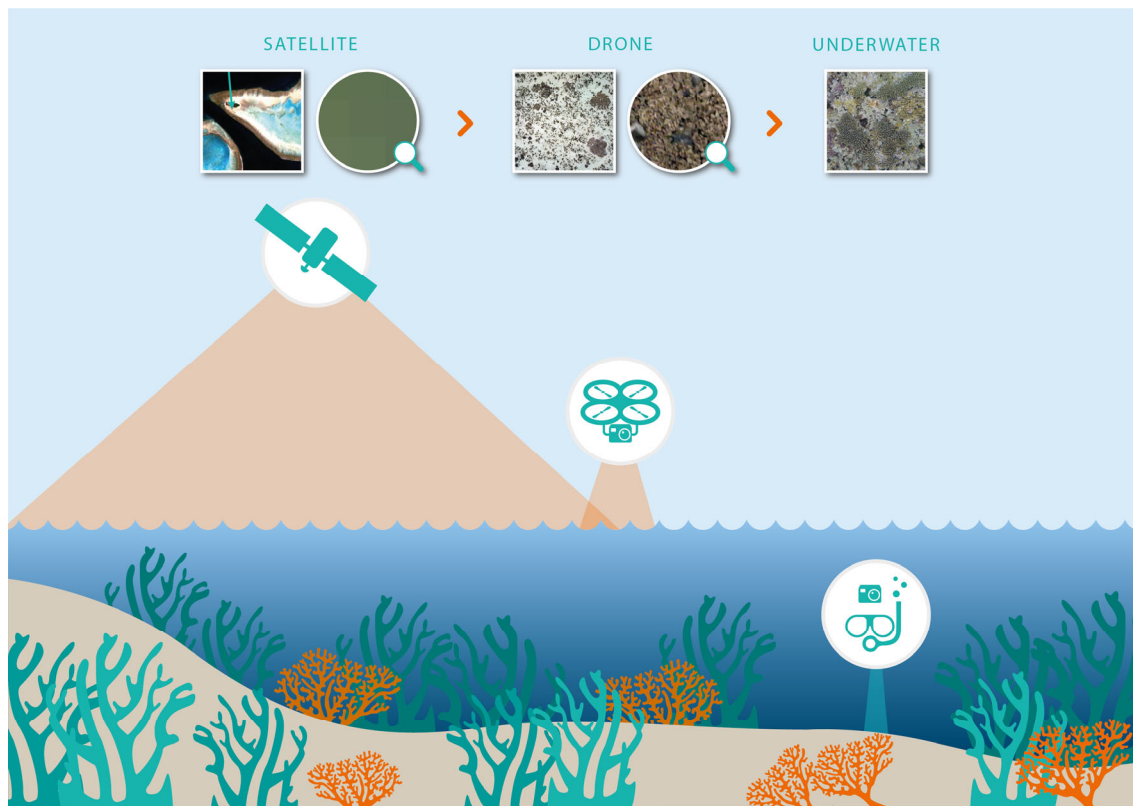
604 <jrn>Wallace, L., Lucieer, A., Watson, C., and Turner, D. (2012). Development of a UAV–LIDAR system with
605 application to forest inventory. *Remote Sensing* **4**(6), 1519–1543. [doi:10.3390/rs4061519](https://doi.org/10.3390/rs4061519)</jrn>

606 <jrn>Watts, A. C., Ambrosia, V. G., and Hinkley, E. A. (2012). Unmanned aircraft systems in remote sensing
607 and scientific research: classification and considerations of use. *Remote Sensing* **4**(6), 1671–1692.
608 [doi:10.3390/rs4061671](https://doi.org/10.3390/rs4061671)</jrn>

609 <jrn>Woodget, A. S., Carbonneau, P. E., Visser, F., and Maddock, I. P. (2015). Quantifying submerged fluvial
610 topography using hyperspatial resolution UAS imagery and structure from motion photogrammetry. *Earth*
611 *Surface Processes and Landforms* **40**(1), 47–64. [doi:10.1002/esp.3613](https://doi.org/10.1002/esp.3613)</jrn>

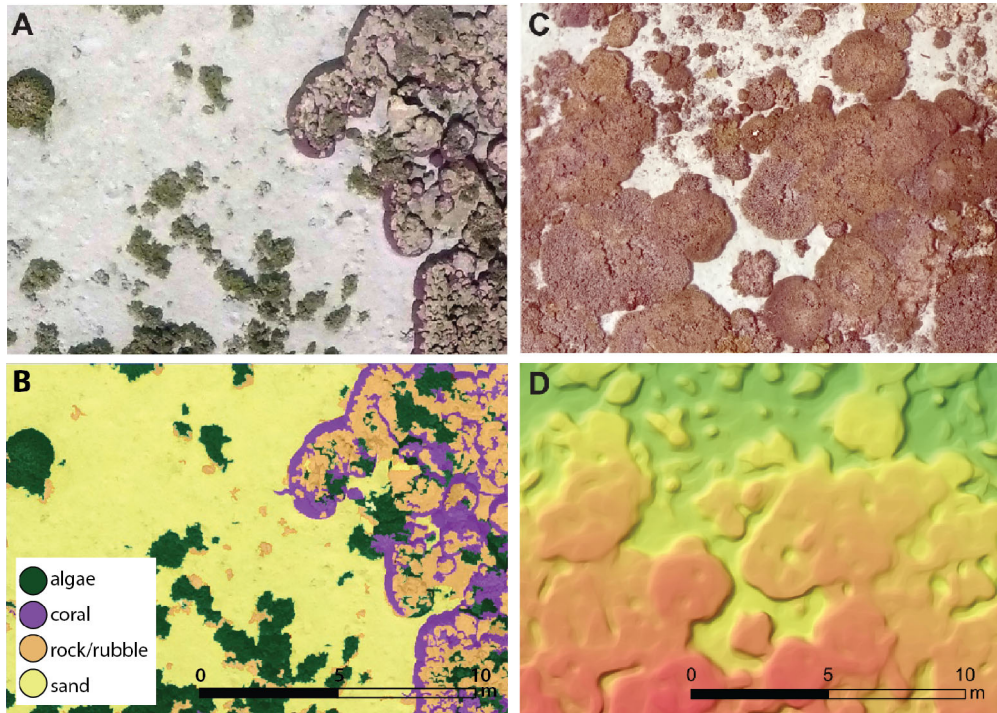
612 <jrn>Xiang, H., and Tian, L. (2011). Development of a low-cost agricultural remote sensing system based on an
613 autonomous unmanned aerial vehicle (UAV). *Biosystems Engineering* **108**(2), 174–190.
614 [doi:10.1016/j.biosystemseng.2010.11.010](https://doi.org/10.1016/j.biosystemseng.2010.11.010)</jrn>

615



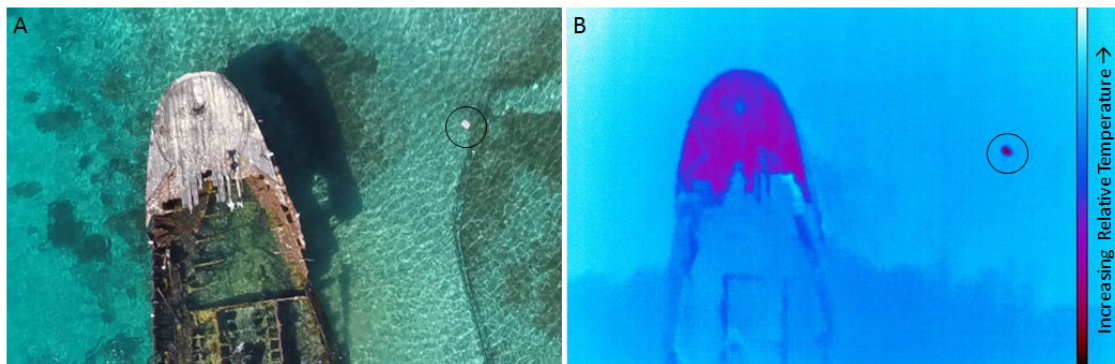
616

617 **Fig. 1.** Varying areas of coverage and scales of observation based on satellite, drone and underwater
618 photography. Image capture altitude is proportional to the area covered and inversely proportional to the level of
619 detail achieved.



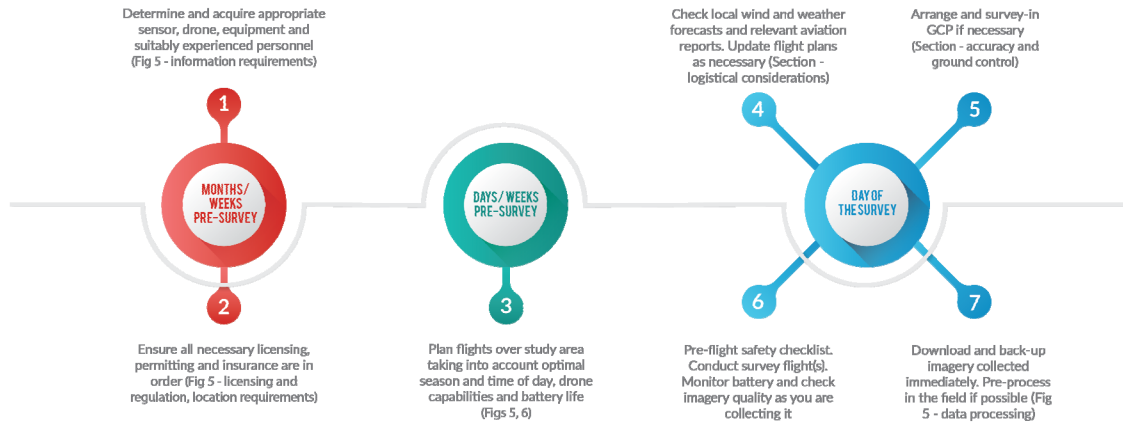
620

621 **Fig. 2.** Using high spatial resolution imagery (*a*, *c*) to derive benthic composition (*b*) surface structure from
622 which to calculate rugosity (*d*). The colour ramp shown in (*c*) is for visual reference only and has not been
623 calibrated to actual depth or structural values.



624

625 **Fig. 3.** Comparison of imagery acquired from (*a*) a drone-based day-time visible Sony a7R digital single-lens
626 reflex camera (Sydney, NSW, Australia) and (*b*) a night-time thermal FLIR a65 camera (Wilsonville, OR, USA).
627 Note that the bright feature circled is a calibration thermometer and buoy. Thermal imagery is captured at 0400
628 hours for optimal results from an altitude of 60 m. A cooler body of water is clearly seen in the bottom portion
629 of the thermal image.



630

631 **Fig. 4.** Drone data collection workflow showing Steps 1–7 and the estimated time frame for each step. GCP,
632 ground control point.



INFORMATION REQUIREMENTS

WHAT IS YOUR FEATURE OF INTEREST?	The level detail required to identify and quantify targets of interest will affect the sensor chosen for the job. For example, measuring a biophysical variable such as chlorophyll content is likely to require a more sophisticated sensor than one used for mapping the difference between corals and sediment.
HOW BIG IS YOUR FEATURE OF INTEREST?	Small features require low altitude flight – aim for a pixel size 1/10 the size of the feature of interest (also see Figure 2).
OVER WHAT SIZE AREA DOES YOUR FEATURE OF INTEREST OCCUR?	Large areas (>200 ha) may be more suited to satellite data, or fixed wing instead of multi-rotor systems (see also Figure 1). Battery life (normally 10-30 minutes for small drones) and line of sight restrictions limit the area that can be covered in any one flight.
IS IT EASY TO IDENTIFY USING HUMAN EYESIGHT OR DOES IT BLEND WITH ITS SURROUNDS?	May need to consider multi-spectral or even thermal imaging. Different drones have different recommended payloads. Some drones may be flexible with payload offerings, others not. Payload type and weight will also impact licensing requirements and insurance costs.
DOES IT LOOK DIFFERENT AT DIFFERENT TIMES OF THE YEAR / SEASON / DAY (E.G. FLOWERING, LEAF COLOUR)?	May impact on timing of surveys. Consider also the necessary additional license exemptions to fly at night time.



LICENSING AND REGULATIONS

DO ANY OF YOUR EMPLOYEES HAVE THEIR REMOTE PILOT'S LICENSE?	Licenses are no longer necessary in Australia for flying craft weighing <2 kg, but insurance may be challenging without a license.
HAVE YOU CONSIDERED A REMOTE AIRCRAFT OPERATOR'S CERTIFICATE (REOC - IF IN AUSTRALIA)?	Once an expensive venture, this is now relatively easy to obtain and will allow you to apply for exemptions to some of the regulations, as well as access public liability insurance.
DO YOU HAVE PUBLIC LIABILITY INSURANCE?	Many insurance companies will insure the drone itself, but consider your requirement to insure for damages in the event of an accident.



LOCATION REQUIREMENTS

ARE THERE ANY AVIATION RESTRICTIONS IN THE AREA IN WHICH YOU HOPE TO FLY (E.G. CLOSE TO AIRPORTS, APPROACH PATHS, MILITARY ZONES, POPULOUS AREAS...)?	May need to lodge exemption applications (only possible if your organisation holds a ReOC)
WILL YOU BE WORKING IN A NATIONAL PARK, MARINE PARK, OR LOCAL COUNCIL AREA?	May need a permit.
WILL YOU BE ABLE TO LAUNCH AND RECOVER CLOSE TO THE SURVEY AREA?	Line of sight regulations restrict the distance that drones can be flown. A long flight distance to the starting point of the survey will limit the size of the survey area itself. Visual obstructions such as hills and trees will also impact on drone visibility.
IS THE SIZE OF THE LAUNCH AND RECOVERY AREA SUFFICIENT FOR YOUR CRAFT TYPE?	Fixed wings require large areas – maybe consider rotary or vertical take-off and land (VTOL) options.



DATA PROCESSING

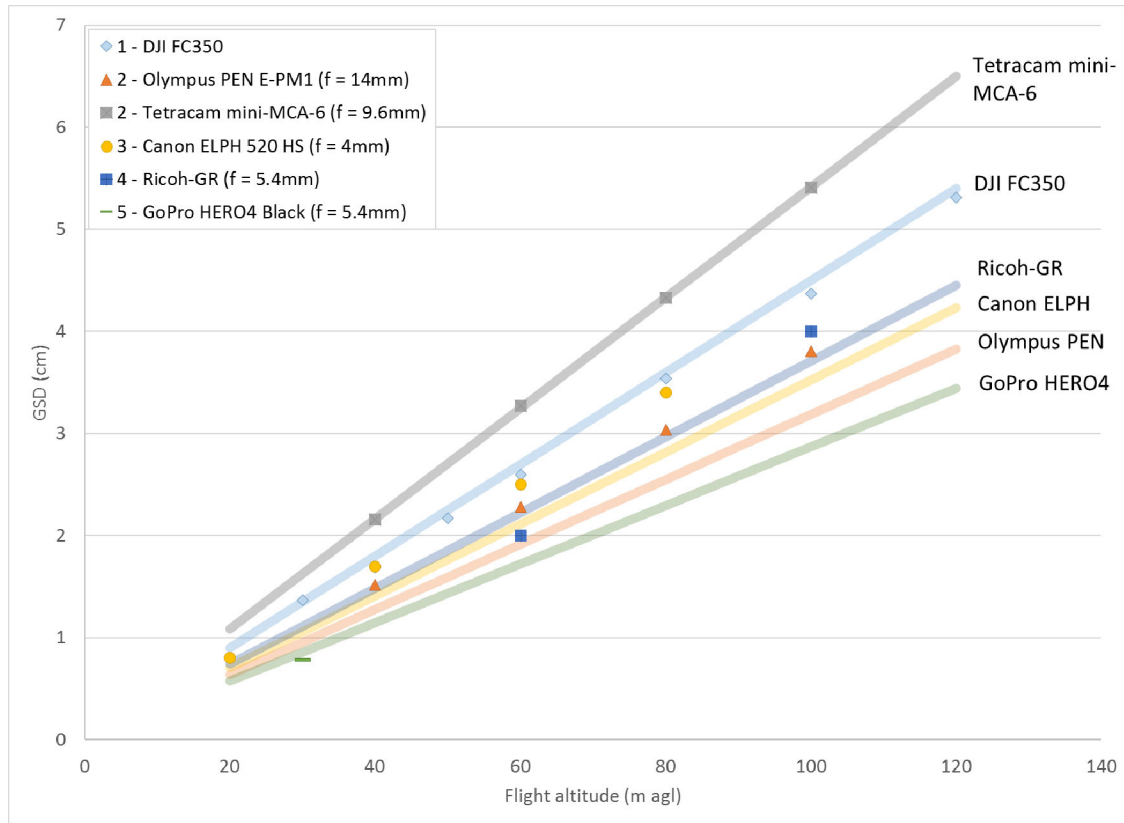
HARDWARE	Access to computing power and data storage for data processing.
DO YOU HAVE ACCESS TO REMOTE SENSING AND GIS SOFTWARE?	Consider cost of licensing to process and analyse the data, or possibility of open source or for service cloud-based options.
DO YOUR STAFF HAVE AN APPROPRIATE LEVEL OF TRAINING PLANNING AND EXECUTING A MISSION, AS WELL AS CONDUCTING THE ANALYSIS?	Consider investing in staff professional development or outsourcing.



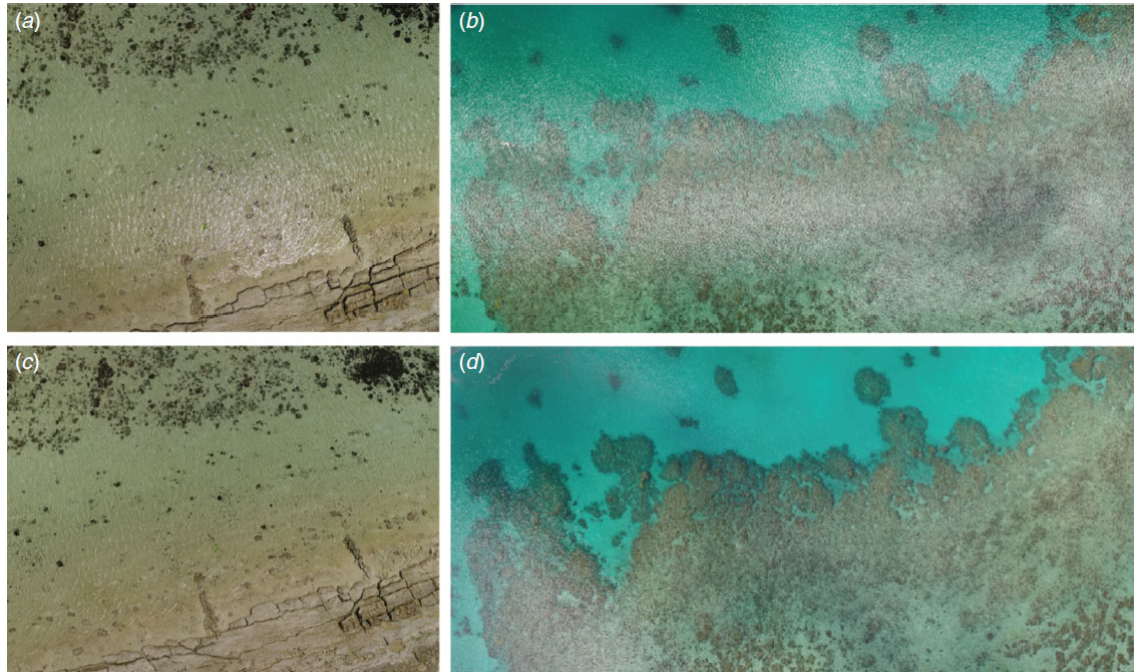
OTHER ADMIN AND LOGISTICS

WHAT IS YOUR TIMELINE FOR TRIALLING AND IMPLEMENTING A SOLUTION?	Purchasing equipment can be done relatively rapidly. Setting up staff training and workflows will take considerably longer.
WHAT IS YOUR BUDGET?	Consider redundancies; spare batteries and chargers; additional accessories such as landing pads, tablets, personal protective equipment; training, insurance, licensing.

634 **Fig. 5.** Defining your drone capability requirements. Note that the regulations listed here are current at the date
635 of submission, although readers should always confirm with the local aviation safety body in their country of
636 operation. In Australia, this is the Civil Aviation Safety Authority.

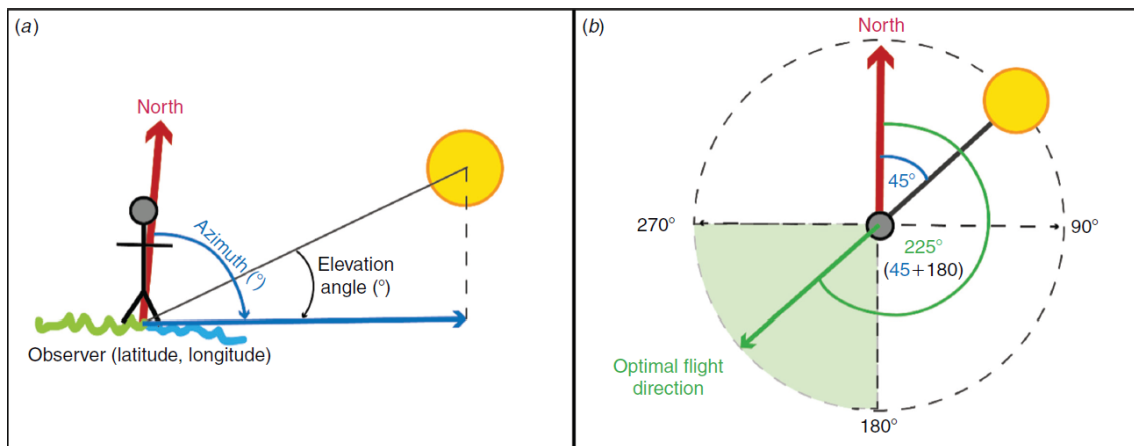


637
638 **Fig. 6.** The ground sampling distance (GSD) achieved with a given sensor at different flight altitudes as
639 reported in the literature. Lines show the theoretical GSD calculated based on the focal length (f) of the sensor.
640 Data are from: 1, [Perroy et al. \(2017\)](#); 2, [Pena et al. \(2015\)](#); 3, [Dandois et al. \(2015\)](#); 4, [Chiabrando et al.](#)
641 [\(2011\)](#); 5, Casella et al. (2017) (GoPro, San Mateo, CA, USA). AGL, above ground level.



642

643 **Fig. 7.** (a, c) Images taken at the same location at 40 m altitude at mid-day at Heron Reef. The image in (a),
644 which is affected by sun glint, was taken with the camera at nadir, whereas the image in (c) was taken with the
645 camera angled slightly off nadir, and the sun glint is minimised. (b, d) A mosaic of the same area of Ellison
646 Reef. In (c), the area was surveyed between 1320 and 1330 hours with the camera at nadir, whereas in (d) the
647 image was surveyed between 1420 and 1430 hours with the camera slightly off nadir.



648

649 **Fig. 8.** (a) Solar azimuth and elevation angle at an observer's location are defined with respect to north. (b)
650 How to plan the optimal flight direction to minimise sun glint in imagery captured over water based on the sun
651 azimuth at your location and time.

652